Chemical Science

ROYAL SOCIETY OF CHEMISTRY

COMMENT

View Article Online
View Journal

Cite this: DOI: 10.1039/d5sc08089d

Reply to the 'Comment on "Mapping photoisomerization dynamics on a three-state model potential energy surface in bacteriorhodopsin using femtosecond stimulated Raman spectroscopy"' by I. Schapiro, M. Olivucci, K. Heyne and S. Haacke, *Chem. Sci.*, 2025, 16, DOI: 10.1039/D5SC05038C

Ziyu Wang,†[a] Boxiang Liu,†[b] Hongjie Li *[b] and Weimin Liu *[a]

Received 20th October 2025
Accepted 16th November 2025

DOI: 10.1039/d5sc08089d

rsc.li/chemical-science

We appreciate the insightful comments by Dr Schapiro *et al.* on our recent article (*Chem. Sci.*, 2025, **16**, 3713). Their comment raises valuable points concerning the excitation regime employed in our femtosecond stimulated Raman spectroscopy (FSRS) experiments, the interpretation of the newly observed 1820 cm^{-1} vibronic band, and the electronic-state assignments of the I and J intermediates in the photoisomerization of bacteriorhodopsin (bR). In this reply, we provide detailed clarifications, supplementary analyses, and additional experimental evidence to address these concerns. These results reinforce the validity of our FSRS interpretation of the AT-PSBR photoisomerization dynamics and clarify the photochemical roles of the I and J intermediates in the retinal protein photocycle.

1 Assessment of excitation regime: single-photon *vs.* multiphoton processes

In our experiments, the laser operated at a repetition rate of 1 kHz, with an actinic pulse duration of 80 fs, and the excitation beam was focused to a spot diameter of ~150 μm on the sample. The corresponding excitation power densities were approximately 3.5 GW cm^{-2} and 14.2 GW cm^{-2} for pulse energies of 50 nJ and 200 nJ, respectively. To evaluate the percentage of protein excited, $P = n_{ph}\sigma$, where n_{ph} is photon density and $\sigma = \sim 2.3 \times 10^{-16}$ cm^2 is the absorption cross section at pump wavelength (as reported in ref. 1). Using these parameters, we obtained the percentage of protein excited $P = 0.19$ and $P = 0.75$ photons per molecule under low (3.5 GW cm^{-2}) and high (14.2 GW cm^{-2}) excitation conditions, respectively.

For the low-intensity excitation ($P \approx 0.19$, 3.5 GW cm^{-2}), the fraction of excited proteins is well below the threshold of $P \approx 0.3$, which defines the low-light excitation regime typically used in bR photodynamic studies.[1] Even under high-intensity excitation ($P \approx 0.75$, 14.2 GW cm^{-2}), the power density remains far below the level required to induce multiphoton effects in the all-*trans* retinal protonated Schiff base (AT-PSBR). Indeed, multiphoton excitation of AT-PSBR has been reported only under extremely high intensities (~180 GW cm^{-2}) or excitation probabilities approaching $P \approx 40$,[1,2] leading to resonant $S_0 \rightarrow S_n$ excitation and an ultrafast (<150 fs) transient decay component, features that are not observed in our measurements. Our high-excitation condition (14.2 GW cm^{-2}) is comparable to the 30–60 GW cm^{-2} range used in ref. 2, where two-photon absorption was shown to selectively excite the tryptophan (Trp86) residue near the retinal chromophore. This process extended the J-state lifetime from 4.5 ps to 9.1 ps due to enhanced excitonic coupling between Trp86 and retinal.[3] Importantly, this reversible effect does not indicate protein damage: after dark recovery overnight, the J-intermediate lifetime returned to 4.5 ps under low-intensity excitation (3.5 GW cm^{-2}).[3]

Given that our excitation intensities (3.5–14.2 GW cm^{-2}) are well below the threshold of multiphoton excitation of AT-PSBR, the observed Raman signal should scale linearly with excitation power. To verify this, we further performed power-dependent FSRS measurements on the bR homolog Archaerhodopsin-3 (AR3) from the halobacterium *Halorubrum sodomense*, as discussed below in Section 3.

[a]*School of Physical Science and Technology, ShanghaiTech University, Shanghai 201210, China. E-mail: liuwm@shanghaitech.edu.cn*

[b]*Center for Transformative Science, School of Life Science and Technology, and Shanghai Clinical Research and Trial Center, ShanghaiTech University, Shanghai 201210, China. E-mail: lihj1@shanghaitech.edu.cn*

† These authors contributed equally to this work.

2 Revisiting the symmetry and electronic origin of the 1820 cm^{-1} vibronic coupling mode

We thank the authors of the Comment for recognizing that "the observation of the 1820 cm^{-1} vibronic band is a clear new experimental finding".[4] They argue, however, that this band cannot be explained by the symmetric polyene model since the structurally distorted AT-PSBR chromophore in bR lacks ideal C_{2h} symmetry. In practice, most naturally occurring long-chain polyenes (*e.g.*, retinals and carotenoids) deviate from perfect C_{2h} symmetry, yet their photophysical behaviors can still be rationalized within the conceptual framework of idealized C_{2h}-symmetric polyenes. For example, in the light-harvesting complex II (LHCII) of higher plants, all-*trans* carotenoids adopt twisted conformations[5] but still exhibit excited-state Raman bands near 1800 cm^{-1}, assigned to C=C stretching vibronic coupling modes.[6,7] Similarly, Kennis *et al.* investigated the structural dynamics of a highly distorted, unprotonated retinal Schiff base in a UV-absorbing rhodopsin using FSRS and observed a comparable C=C stretching vibronic coupling mode, even though this isomer displays a strongly asymmetric and polarized π-electron distribution.[8] Our own results, together with these previous findings, suggest that although the molecular symmetry of AT-PSBR does not fully conform to that of linear polyenes, the essential A_g^- and B_u^+ character of their excited-state manifolds remains largely valid, as confirmed by structure-based calculations for protonated AT-PSBR.[9] In the excited state, dynamic torsional motion further breaks the C_{2h} symmetry, leading to a reduction in the intensity of the C=C vibronic coupling mode, which ultimately vanishes following photoisomerization and the formation of ground-state photoproducts.[8] This interpretation is consistent with our FSRS observations in bR, where the double-exponential decay of the 1820 cm^{-1} vibronic band reflects the presence of two excited intermediates (I and J) that remain in non-*cis* configurations prior to photoisomerization.

Building on this discussion, Dr Schapiro *et al.* emphasize that the I state possesses a mixed $2A_g^-/1B_u^+$ character, rather than arising from $2A_g^-/1A_g^-$ vibronic coupling. In ref. 7 cited in the Comment (ref. 11 in our reply), two-dimensional electronic photon echo (2DPE) spectroscopy revealed pronounced oscillatory features around 100 fs. Based on their newly proposed three-state model, the population on the S_1 state was suggested to pass through two avoided crossings between S_1 and S_2, rather than a single one as assumed in the original three-state model,[10,11] thereby endowing S_1 with a charge-transfer ($1B_u^+$) character. Consequently, the observed oscillations were assigned to the coherent mixing between the S_2 ($2A_g^-$) and S_1 ($1B_u^+$) states, with characteristic frequency components at 945 and 1634 cm^{-1}. In our FSRS experiments, however, the observation of a $2A_g^-/1A_g^-$ vibronic coupling Raman mode at 1820 cm^{-1} for both the I and J states supports the traditional three-state model, in which the S_2 ($2A_g^-$) state forms an avoided crossing with S_1 ($1B_u^+$). At this crossing, the wavefunction characters of S_1 (charge transfer) and S_2 (diradical) states exchange, leading the populated state to acquire a $2A_g^-$ like character as the system approaches the conical intersection. We further note that even within the original three-state framework, the avoided crossing naturally narrows the S_2/S_1 energy gap, giving rise to a mixed $2A_g^-/1B_u^+$ character. Additionally, in the 2DPE study, the pronounced oscillations were observed only under 540 nm excitation and disappeared when the excitation wavelength was shifted to 570 nm.[11] In our FSRS experiments, the actinic pump was set at 570 nm, which likely explains the absence of observable S_2/S_1 diabatic mixing in our results. Future FSRS measurements using a 540 nm pump could provide further insight into this diabatic coupling behavior.

Finally, regarding the nature of the J state, Dr Schapiro *et al.* state in their Comment that "according to many papers on bR, J is identified as a vibrationally excited ground state population."[4] However, the assignment of the J state, whether it represents an excited-state or ground-state species, remains under debate. Indeed, a series of theoretical and computational studies have assigned the J intermediate to a vibrationally hot ground-state species formed immediately after the decay of the excited I state,[12,13] and this interpretation has also been supported by several time-resolved experimental investigations.[11,14–16] In contrast, a theoretical study by Birge and co-workers proposed that the J intermediate possesses an electronically excited character,[17] and this view was subsequently reinforced by a series of ultrafast spectroscopic studies providing experimental evidence that J retains excited-state features.[1,18–22] In our experiments, the observation of a τ_2 component associated with the 1820 cm^{-1} vibronic coupling mode provides direct evidence of $2A_g^-$ character in the J state, supporting its assignment as an excited-state intermediate rather than a vibrationally hot ground-state species in bR.

3 Experimental validation of the FSRS interpretation through Archaerhodopsin-3

To further substantiate the validity of our FSRS interpretation of the AT-PSBR structural dynamics, particularly the assignment and photochemical roles of the I and J intermediates, we have conducted additional FSRS experiments on a related microbial rhodopsin system, AR3. This protein shares the same retinal chromophore as bR but exhibits distinct hydrogen bond network and structural environments within its binding pocket (see Fig. 1a). Importantly, AR3 has been extensively characterized by Dr Haacke *et al.* in their recent work,[23] providing a well-established reference framework for comparison.

As depicted in Fig. 1c, upon photoexcitation at 570 nm (200 nJ, 14.2 GW cm^{-2}, $P \approx 0.56$), the FSRS spectra of the light-adaptive state AR3 reveal Raman peaks at 1530 cm^{-1} (C=C stretching), 1700 cm^{-1} (C=N stretching), and 1835 cm^{-1}. Analogous to bR, this 1835 cm^{-1} is attributed to the C=C stretching $2A_g^-/1A_g^-$ vibronic coupling mode. The transient amplitude of the C=C stretching (1530 cm^{-1}) mode is fitted with three decay components of $\tau_1 = 300$ fs, $\tau_2 = 1.7$ ps, and $\tau_3 =$ an infinitely long lifetime (Fig. 1d), reflecting the sequential formation and relaxation of

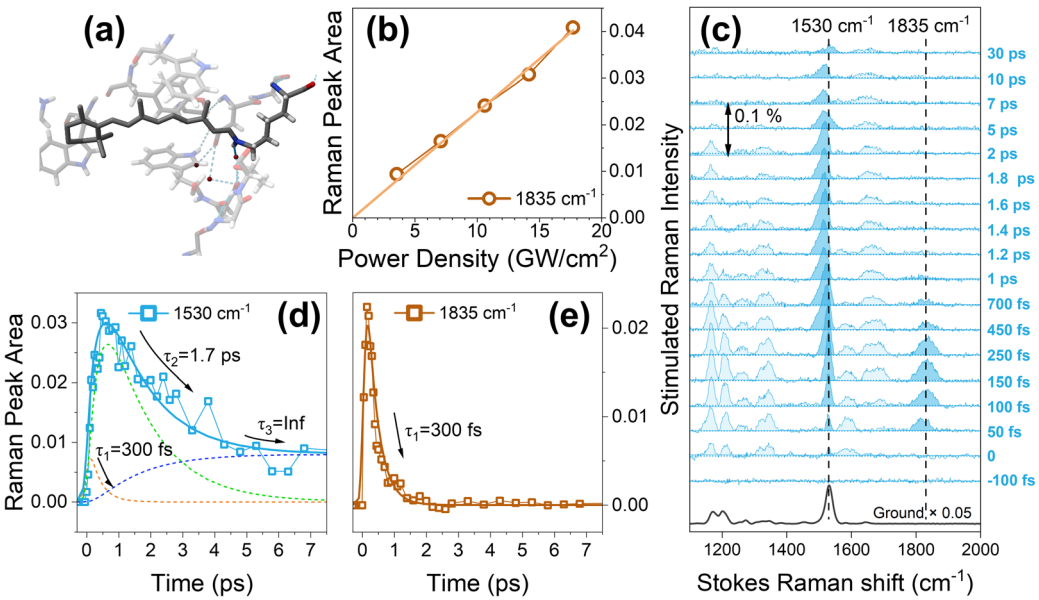

Fig. 1 (a) A schematic diagram illustrating the AT-PSBR chromophore of AR3 and its surrounding protein environment (PDB code 6S6C); (b) excitation power dependence of the Raman mode intensities at 1835 cm^{-1} in AR3; (c) FSRS spectra of AT-PSBR in AR3 at an excitation energy of 200 nJ per pulse, the ground state FSRS spectrum is shown at the bottom for comparison; transient Raman intensities of the 1530 cm^{-1} (d) and 1835 cm^{-1} (e) Raman modes in AR3.

intermediates I, J, and K. In contrast, the transient amplitude of the 1835 cm^{-1} mode in AR3 exhibits a single exponential decay of $\tau_1 = 300$ fs (Fig. 1e), indicating that this short-lived component primarily arises from excited state decay (I state) along the isomerization, followed by the formation of the hot *cis* ground state (J state) photoproduct (τ_2).[23] These results are fully consistent with previous time-resolved spectroscopic studies of AR3.[23] Unlike in bR, where the vibronic coupling mode persists through both the I and J intermediates, reflecting a two-step C13=C14 bond twisting process approaching a ~90° torsion, AR3 shows a much faster decay of this vibronic feature. The difference originates from variations in the local electrostatic environment and hydrogen-bonding network surrounding the Schiff base in bR and AR3, which modulate the excited-state potential energy landscape.

To ensure that the excitation fluence used in our measurements does not induce multiphoton effects in the AT-PSBR of AR3, we performed excitation power-dependent FSRS experiments over a range of excitation intensities from 3.54 GW cm^{-2} ($P \approx 0.14$) to 17.68 GW cm^{-2} ($P \approx 0.70$). As shown in Fig. 1b, the integrated intensities of 1835 cm^{-1} Raman bands at $t = 100$ fs scale linearly with excitation energy. This linear dependence confirms that the photoexcitation process proceeds *via* one-photon absorption rather than a multiphoton excitation pathway in the AT-PSBR chromophore of AR3. Consequently, our results demonstrate that the observed vibronic coupling features originate from the linear, single-photon excitation regime, ensuring that the reported structural dynamics and Raman-active modes are directly comparable with well-established ultrafast studies on retinal proteins.

In summary, the control experiments on AR3 confirm that the vibronic coupling signatures observed in our FSRS measurements originate from a linear, single-photon excitation regime. The observed 1820 cm^{-1} vibronic band in bR and 1835 cm^{-1} in AR3 originate from C=C stretching vibronic coupling between the $2A_g^-$ and $1A_g^-$ manifolds, reflecting the transient evolution of the *trans*-excited intermediate before *cis* ground-state photoproduct formation. The comparison of bR with AR3 highlights that variations in local protein environment modulate the *trans–cis* isomerization without altering the fundamental three-state photoisomerization framework. These findings strengthen the mechanistic understanding of retinal photoisomerization revealed by FSRS.

Author contributions

Z. W. and W. L. conceived, designed and performed the experiments. Z. W. analyzed the experimental results. Z. W., H. L. and W. L. co-wrote the manuscript. B. L. and H. L. provided the AR3 samples. All authors participated in discussions and edited the manuscript. W. L. directed the project.

Conflicts of interest

There are no conflicts of interest to declare.

Data availability

The authors confirm that the data supporting the findings of this study are available within the article.

Acknowledgements

This work was supported by the National Natural Science Foundation of China (No. 22373068); the Double First-Class Initiative Fund of ShanghaiTech University; ShanghaiTech

Start-up Funding (F-0201-16-006); Shanghai Pujiang Program (24PJA082); Natural Science Foundation of Shanghai (25ZR1404007).

References

1 B. Schmidt, C. Sobotta, B. Heinz, S. Laimgruber, M. Braun and P. Gilch, Excited-state dynamics of bacteriorhodopsin probed by broadband femtosecond fluorescence spectroscopy, *Biochim. Biophys. Acta Bioenerg.*, 2005, **1706**, 165–173.

2 G. Nass Kovacs, J.-P. Colletier, M. L. Grünbein, Y. Yang, T. Stensitzki, A. Batyuk, S. Carbajo, R. B. Doak, D. Ehrenberg and L. Foucar, Three-dimensional view of ultrafast dynamics in photoexcited bacteriorhodopsin, *Nat. Commun.*, 2019, **10**, 3177.

3 Z. Wang, Y. Chen, J. Jiang, X. Zhao and W. Liu, Mapping photoisomerization dynamics on a three-state model potential energy surface in bacteriorhodopsin using femtosecond stimulated Raman spectroscopy, *Chem. Sci.*, 2025, **16**, 3713–3719.

4 I. Schapiro, M. Olivucci, K. Heyne and S. Haacke, Comment on "Mapping photoisomerization dynamics on a three-state model potential energy surface in bacteriorhodopsin using femtosecond stimulated Raman spectroscopy" by Z. Wang, Y. Chen, J. Jiang, X. Zhao and W. Liu, *Chem. Sci.*, 2025, **16**, 3713, *Chem. Sci.*, 2025, **16**, DOI: 10.1039/D5SC05038C.

5 M. Ruan, H. Li, Y. Zhang, R. Zhao, J. Zhang, Y. Wang, J. Gao, Z. Wang, Y. Wang and D. Sun, Cryo-EM structures of LHCII in photo-active and photo-protecting states reveal allosteric regulation of light harvesting and excess energy dissipation, *Nat. Plants*, 2023, **9**, 1547–1557.

6 J. M. Artes Vivancos, I. H. Van Stokkum, F. Saccon, Y. Hontani, M. Kloz, A. Ruban, R. van Grondelle and J. T. Kennis, Unraveling the excited-state dynamics and light-harvesting functions of xanthophylls in light-harvesting complex II using femtosecond stimulated Raman spectroscopy, *J. Am. Chem. Soc.*, 2020, **142**, 17346–17355.

7 T. Ma, M. Ruan, R. Zhao, Z. Wang, Y. Wang, Y. Huang, Y. Weng and W. Liu, Distorted Intermediate S_X ($1B_u^-$) State in Xanthophylls Drives Efficient Energy Transfer in Light-Harvesting Complex II, *J. Phys. Chem. Lett.*, 2025, **16**, 6711–6718.

8 Y. Hontani, M. Broser, M. Luck, J. Weißenborn, M. Kloz, P. Hegemann and J. T. Kennis, Dual photoisomerization on distinct potential energy surfaces in a UV-absorbing rhodopsin, *J. Am. Chem. Soc.*, 2020, **142**, 11464–11473.

9 M. d. C. Marin, D. Agathangelou, Y. Orozco-Gonzalez, A. Valentini, Y. Kato, R. Abe-Yoshizumi, H. Kandori, A. Choi, K.-H. Jung and S. Haacke, Fluorescence enhancement of a microbial rhodopsin *via* electronic reprogramming, *J. Am. Chem. Soc.*, 2018, **141**, 262–271.

10 W. Humphrey, H. Lu, I. Logunov, H.-J. Werner and K. Schulten, Three electronic state model of the primary phototransformation of bacteriorhodopsin, *Biophys. J.*, 1998, **75**, 1689–1699.

11 S. Gozem, P. J. Johnson, A. Halpin, H. L. Luk, T. Morizumi, V. I. Prokhorenko, O. P. Ernst, M. Olivucci and R. D. Miller, Excited-state vibronic dynamics of bacteriorhodopsin from two-dimensional electronic photon echo spectroscopy and multiconfigurational quantum chemistry, *J. Phys. Chem. Lett.*, 2020, **11**, 3889–3896.

12 G. Haran, K. Wynne, A. Xie, Q. He, M. Chance and R. M. Hochstrasser, Excited state dynamics of bacteriorhodopsin revealed by transient stimulated emission spectra, *Chem. Phys. Lett.*, 1996, **261**, 389–395.

13 J. Herbst, K. Heyne and R. Diller, Femtosecond infrared spectroscopy of bacteriorhodopsin chromophore isomerization, *Science*, 2002, **297**, 822–825.

14 R. A. Mathies, C. Brito Cruz, W. T. Pollard and C. V. Shank, Direct observation of the femtosecond excited-state cis-trans isomerization in bacteriorhodopsin, *Science*, 1988, **240**, 777–779.

15 D. Xu, C. Martin and K. Schulten, Molecular dynamics study of early picosecond events in the bacteriorhodopsin photocycle: dielectric response, vibrational cooling and the J, K intermediates, *Biophys. J.*, 1996, **70**, 453–460.

16 J. K. Yu, R. Liang, F. Liu and T. J. Martínez, First-principles characterization of the elusive I fluorescent state and the structural evolution of retinal protonated Schiff base in bacteriorhodopsin, *J. Am. Chem. Soc.*, 2019, **141**, 18193–18203.

17 R. R. Birge, L. A. Findsen and B. M. Pierce, Molecular dynamics of the primary photochemical event in bacteriorhodopsin. Theoretical evidence for an excited singlet state assignment for the J intermediate, *J. Am. Chem. Soc.*, 1987, **109**, 5041–5043.

18 K. Hasson, F. Gai and P. A. Anfinrud, The photoisomerization of retinal in bacteriorhodopsin: experimental evidence for a three-state model, *Proc. Natl. Acad. Sci. U. S. A.*, 1996, **93**, 15124–15129.

19 G. Atkinson, L. Ujj and Y. Zhou, Vibrational spectrum of the J-625 intermediate in the room temperature bacteriorhodopsin photocycle, *J. Phys. Chem. A*, 2000, **104**, 4130–4139.

20 S. L. Logunov, V. V. Volkov, M. Braun and M. A. El-Sayed, The relaxation dynamics of the excited electronic states of retinal in bacteriorhodopsin by two-pump-probe femtosecond studies, *Proc. Natl. Acad. Sci. U. S. A.*, 2001, **98**, 8475–8479.

21 J. Wang and M. A. El-Sayed, Time-resolved long-lived infrared emission from bacteriorhodopsin during its photocycle, *Biophys. J.*, 2002, **83**, 1589–1594.

22 M. Macernis, L. Mourokh, L. Vinciunas and L. Valkunas, Mechanism of proton transfer in bacteriorhodopsin, *Lith. J. Phys.*, 2022, **62**, 179–193.

23 K. Herasymenko, D. Walisinghe, M. Konno, L. Barneschi, I. de Waele, M. Sliwa, K. Inoue, M. Olivucci and S. Haacke, Archaerhodopsin 3 is an ideal template for the engineering of highly fluorescent optogenetic reporters, *Chem. Sci.*, 2025, **16**, 761–774.

